Exfoliation and Reassembling Route to Mesoporous Titania Nanohybrids

Seung-Min Paek,[†] Hyun Jung,[†] Young-Jun Lee,[†] Man Park,[†] Seong-Ju Hwang,*[,‡] and Jin-Ho Choy*[,‡]

School of Chemistry and Molecular Engineering, Seoul National University, Seoul 151-747, Korea, and Center for Intelligent Nano-Bio Materials (CINBM), Division of Nanoscience and Department of Chemistry, Ewha Womans University, Seoul 120-750, Korea

Received October 4, 2005. Revised Manuscript Received December 6, 2005

To fabricate mesoporous photocatalysts with delaminated structure, the exfoliated layered titanate in aqueous solution was reassembled in the presence of anatase TiO_2 nanosol particles to induce a great number of mesopores and eventually a large surface area of TiO_2 photocatalysts. No (0*l*0) peaks corresponding to the layered titanate appear in the X-ray diffraction patterns of the reassembled hybrids, which suggests that the titanate nanosheets were randomly hybridized with TiO_2 nanoparticles without any restacking into the layered phase. According to the high-resolution transmission electron microscopy images of these nanohybrids, the randomly oriented titanate nanosheets can be seen clearly along with TiO_2 nanosol particles with spherical images, indicating that the exfoliated sheets are indeed incorporated with anatase nanosol particles to form porous materials. From N_2 adsorption−desorption isotherms, these nanohybrids are fairly high in specific surface area and in mesoporosity for effective photocatalysis (S_{BET} = ∼190 m^2/g, pore size = ∼6 nm). The photocatalytic activity of the present mesoporous nanohybrids is superior to that of TiO_2 nanosol particles or layered titanate alone in terms of the degradation of organic pollutants such as 4-chlorophenol, methyl orange, and methylene blue.

Introduction

Titanium dioxide has been widely used in a broad range of important fields such as photocatalysts, photovoltaic cells, electronic devices, and sensors. Although its photoresponsive performance is primarily governed by the crystalline phases with semiconducting properties,[1−4] the textural properties also exert profound effects. In fact, more attention has been given to control the size and shape of primary particles as well as to manipulate their arrangement and network structure. In particular, incessant attempts have focused on tailoring the mesoporous network with high surface area because this type of network structure could promise optimal performance in photoresponsive applications such as photocatalysis and dye-sensitized solar cell.[5,6] The mesoporous structure with high surface area could provide not only easy accessibility of guest molecules to active sites but also more chances to receive both light and guest molecules. Therefore, several attempts have been made recently to realize the mesoporous transition metal oxides by using organic templates such as phosphates and amines, which resulted in very high specific surface area.[7−10] However, after the surfactants are removed by solvent extraction and/or calcination, the mesostructure becomes quite unstable as a result of the amorphous nature of the pore walls,[11] and it was also found that even the phosphate-assisted approach gave rise to an increase of titanium oxo-phosphate linkage resulting in thermal instability. To overcome such an inevitable drawbacks, a nanohybridization between nanoparticles and inorganic nanosheets as stabilizer and support has been suggested to optimize the stability of mesoporous sturucture and the performance of semiconducting functions, and we have made several attempts to intercalate anatase nanoparticles into layered titanates, which led to a significant enhancement of photocatalytic activity despite their microporous textures.[12,13] In case of water splitting, the micropore is large enough to facilitate water molecules, whereas in the photodecomposition of bulky organic molecules the mesoporous structure is highly required for the access into active sites in photocatalyst. In the present study, we are quite successful in developing a highly mesoporous hybrid composed of anatase

* To whom correspondence should be addressed. Tel.: +82-2-3277-4135. Fax: +82-2-3277-4340. E-mail: jhchoy@ewha.ac.kr.
[†] Seoul National University.
[‡] Ewha Womans University.

(1) Hoffmann, M. R.; Martin, S. T.; Choi, W.; Bahnemann, D. W. *Chem. Rev.* **1995**, *95*, 69.
(2) O'Regan, B.; Gratzel, M. *Nature* **1991**, *353*, 737.
(3) (a) Green, M. *Chem. Ind.* **1996**, *17*, 641. (b) Monk, P. M. S.; Mortimer, R. J.; Rosseinsky, D. R. *Electrochromism: Fundamentals and Applications*; VCH: Weinheim, 1995. (c) Mortimer, R. J. *Chem. Soc. Rev.* **1997**, *26*, 147.
(4) Favier, F.; Walter, E. C.; Zach, M. P.; Benter, T.; Penner, R. M. *Science* **2001**, *293*, 2227.
(5) Serpone, N.; Pelizzetti, E. *Photocatalysis: fundamentals and applications*; Academic Press: New York, 1989.
(6) Kalyanasundaram, K.; Gratzel, M. *Coord. Chem. Rev.* **1998**, *77*, 347.
(7) Antenolli, D. M.; Ying, J. Y. *Angew. Chem., Int. Ed. Engl.* **1995**, *34*, 2014.
(8) Wong, M. S.; Ying, J. Y. *Chem. Mater.* **1998**, *10*, 2067.
(9) Severin, K. G.; Abdel-Fattah, T. M.; Pinnavaia, T. J. *Chem. Commun.* **1998**, 1471.
(10) Antenolli, D. M.; Ying, J. Y. *Chem. Mater.* **1996**, *8*, 874.
(11) Antenolli, D. M. *Microporous Mesoporous Mater.* **1999**, *30*, 315.
(12) Choy, J. H.; Lee, H. C.; Jung, H.; Hwang, S. J. *J. Mater. Chem.* **2001**, *11*, 2232.
(13) Choy, J. H.; Lee, H. C.; Jung, H.; Hwang, S. J.; Kim, H.; Boo, H. *Chem. Mater.* **2002**, *14*, 2486.

10.1021/cm052201d CCC: $33.50
Published on Web 02/03/2006

nanoparticles and exfoliated titanate layers, in which not only the TiO_2 nanoparicles but also the exfoliated nanosheets could play a role as the photocatalyst. Our key strategy in this study is to develop a new hybrid catalyst with thermally stable porous structure that would facilitate both high mesoporosity and surface area by reassembling two-dimensional titanate nanosheets in the presence of anatase nanoparticles without any deterioration of their fundamental crystal structures.[14,15] Thus, the present "pure" titania hybrid shows much superior semiconducting property, especifically in photocatalysis.

Experimental Section

Sample Preparation. The host cesium titanate, $Cs_{0.67}Ti_{1.83}\square_{0.17}O_4$, was prepared by heating a stoichiometric mixture of Cs_2CO_3 and TiO_2 at 800 °C for 20 h. The corresponding protonic form, $H_{0.67}Ti_{1.83}\square_{0.17}O_4 \cdot H_2O$, was obtained by reacting cesium titanate powder with 1 M HCl aqueous solution at room temperature for 3 days. During the proton exchange reaction, the HCl solution was replaced with a fresh one every 24 h. The layered protonic titanate was exfoliated into single titanate sheets by intercalating TBA (tetrabutylammonium) molecules, as reported previously.[16]

On the other hand, TiO_2 colloidal solutions were prepared by hydrolysis of titanium isopropoxide, $Ti(OCH(CH_3)_2)_4$, as follows: Under a stream of dry nitrogen, 62.5 mL of $Ti(OCH(CH_3)_2)_4$ (Aldrich) was mixed with 10 mL of 2-propanol (Carlo erba, 99%). The mixture was slowly added to 0.1 M HNO_3 aqueous solution (375 mL) under vigorous stirring and peptized at 80 °C for 8 h. The mesoporous nanohybrids were prepared by hybridizing exfoliated titanate sheets with anatase nanoparticles. The anatase nanoparticles were slowly added into exfoliated titanate solution to obtain mesoporous materials, in which the Ti ratio (tuning of the Ti ratio $[Ti]_{\text{nanoparticles}}/[Ti]_{\text{layered titanate}} = 1.5$ for nanohybrid-I and 5 for nanohybrid-II) was carefully adjusted from 1.5 to 5.0. After reacting the mixture at room temperature for 24 h, the flocculated product was centrifuged, washed with distilled water, and dried in a vacuum. The obtained nanohybrids were heated at 450 °C for 1 h to complete the grafting reaction. And, for the comparison of photocatalystic activities with the present mesoporous hybrids, TiO_2-pillared layered titanate nanohybrid (hereafter abbreviated as microporous hybrid) with a pore size of ~1 nm was also synthesized and calcined at 300 °C for 2 h as reported previously.[12,13] The detailed procedure for the preparation of the microporous hybrid is described in Supporting Information.

Sample Characterization. The crystal structures for the samples were studied by powder X-ray diffraction (XRD) measurements using Ni-filtered Cu Kα radiation with a Philips PW 1830. High-resolution transmission electron microscopy (HRTEM) images were examined with a Philips CM200 microscope at an accelerating voltage of 200 kV. Thermogravimetry−differential thermal analysis (TG-DTA) was carried out to check the thermal behavior of nanohybrids in an ambient atmosphere where the heating rate was fixed at 5 °C/min. The nitrogen adsorption−desorption isotherms were measured at liquid nitrogen temperature with a gas sorption analyzer (Sorptomatic 1990). The samples were degassed at 150 °C in a vacuum below 10^{-3} Torr for 12 h prior to measurements. Diffuse reflectance UV−vis spectra for the evaluation of photochemical properties were recorded on a Perkin-Elmer Lambda 12 spectrometer equipped with an integrating sphere 60 mm in diameter using $BaSO_4$ as a standard. X-ray absorption near edge structure (XANES) experiments at the Ti K-edge were performed at the beam line 7C in the Pohang Accelerator Laboratory in Korea. XANES data were collected at room temperature in transmission mode using gas-ionization detectors. Data acquisition and analysis were carried out by the standard procedure.[17]

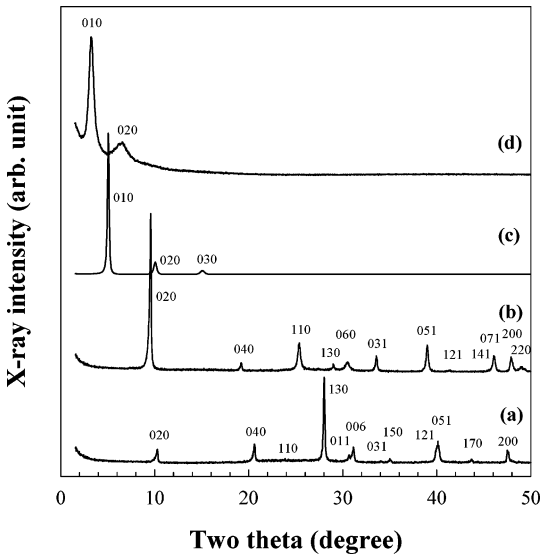

Figure 1. XRD patterns for (a) the layered cesium titanate, (b) layered protonic titanate, (c) TBA-intercalated layered titanate, and (d) microporous hybrid.

Photocatalytic measurements were performed in a Pyrex photoreactor (100 mL) with quartz window. The UV light source for these experiments was accomplished by a Müller 300 W Xe arc lamp (LAX 1530). Light passed through a 10-cm IR water filter, and then the filtered light was focused onto the reactor. Test substrates were 4-chlorophenol (4-CP), methyl orange (MO), and methylene blue (MB). An aqueous solution of 100 mL of test substrate (1.0×10^{-5} M) and 25 mg of catalyst powders were placed in a Pyrex vessel. Prior to irradiation, the suspensions were magnetically stirred in the dark for 2 h to establish adsorption/desorption equilibrium between the organic molecules and the surface of the catalysts. Each sample was at first filtered through a Millipore membrane filter (0.2 μm pores), and the filtrates were analyzed by recording the spectrophotometrical changes in wavelength at the maximal absorption in the UV−vis spectra of the substrates using a Perkin-Elmer Lambda 12 spectrometer.

Results and Discussions

Powder XRD Analysis. The powder XRD pattern for the pristine $Cs_{0.67}Ti_{1.83}\square_{0.17}O_4$ is shown in Figure 1 together with those of the proton-exchanged form $H_{0.67}Ti_{1.83}\square_{0.17}O_4 \cdot H_2O$, TBA-intercalated one, and microporous nanohybrid. The XRD pattern of layered cesium titanate shows the lepidocrocite structure with orthorhombic symmetry. Upon acid treatment, its (020) reflection is shifted toward a lower angle (Figure 1b) as a result of the lattice expansion upon intercalation of water molecules into interlayer space of the layered protonic titanate. For the synthesis of microporous hybrid material, before the ion-exchange reaction with TiO_2

(14) van Olphen, H. *An Introduction to Clay Colloid Chemistry*; Wiley: New York, 1977.
(15) Abe, R.; Shinohara, K.; Tanaka, A.; Hara, M.; Kondo, J. N.; Domen, K. *Chem. Mater.* **1997**, *9*, 2179.
(16) Sasaki, T.; Watanabe, M.; Hashizume, H.; Yamada, H.; Nakazawa, H. *J. Am. Chem. Soc.* **1996**, *118*, 8329.
(17) (a) Teo, B. K. *EXAFS: Basic Principles and Data Analysis*; Springer-Verlag: Berlin, 1986. (b) Paek, S. M.; Jung, H.; Park, M.; Lee, J. K.; Choy, J. H. *Chem. Mater.* **2005**, *17*, 3492.

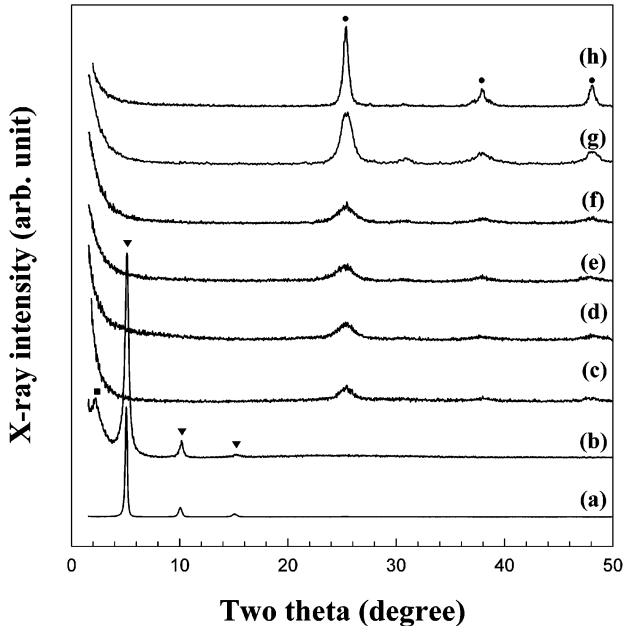

Figure 2. XRD patterns for the samples: (a) Ti ratio = 0 (TBA-intercalated titanate), (b) Ti ratio = 1, (c) Ti ratio = 1.5, (d) Ti ratio = 2.5, (e) Ti ratio = 5, (f) as-prepared TiO_2 nanoparticle, (g) Ti ratio = 1.5 (heat-treated at 450 °C), and (h) TiO_2 nanoparticle (heat-treated at 450 °C; ●, anatase; ▼, TBA-intercalated layered titanate; and ■, anatase-intercalated layered titanate)

nanoparticles, the layered titanate was exfoliated by intercalation of TBA (Figure 1c). As shown in Figure 1d, upon the reaction of the exfoliated titanate with the TiO_2 nanoparticle, the (020) reflection of the protonic form is displaced to the (010) reflection of a microporous hybrid at a lower angle because of the intercalation of the TiO_2 nanoparticle into the interlayer spaces of titanate. Our previous study reveals that TiO_2 nanoparticles with an average size of 1.5 nm are multistacked in the interlayer spaces of titanate to form the microporous pillared hybrid.[12,13]

Figure 2 shows the XRD patterns for the self-restacked titanate along with those for the mesoporous nanohybrids having a variety of Ti ratios ($[Ti]_{nanoparticles}/[Ti]_{layered\ titanate}$). The well-developed (0*l*0) peaks of self-restacked titanate (Ti ratio = 0, Figure 2a) at $2\theta = 5$, 10, and 15° indicate that TBA is intercalated between the titanate sheets to form a turbostatic lamellar structure with the interlayer space of 1.75 nm, as previously reported.[18] When the Ti ratio is less than 1.5 (Ti ratio = 1, Figure 2b), The TBA-intercalated phase and TiO_2-intercalated one become observed, whereas when the Ti ratio is beyond 5 (Figure 2e), the pore size and specific surface area would be decreased because of the agglomeration of excess TiO_2 nanoparticles, which will be discussed in detail in the nitrogen adsorption−desorption section. Therefore, the optimal ratio of titanium could be suggested as 1.5 (nanohybrid-I) to 5.0 (nanohybrid-II). In a region of low angle, the XRD patterns for these mesoporous nanohybrids with the optimal Ti ratio do not show any diffraction peaks resulted from the protonic phase and TBA intercalated phase that could be formed by self-reassembling of exfoliated layers. The diffraction peak centered at $2\theta = 25.4°$ is attributed to the anatase (101) reflection, supporting that the exfoliated layered titanate nanosheets are randomly incorporated into TiO_2 nanoparticle matrixes without forming any self-restacked two-dimensional phase. As shown in Figure 1f, as-prepared TiO_2 nanoparticles used in this study have anatase structure with the mean particle size of 5.4 nm, which is estimated by the Scherrer equation.[19] Figure 2h shows that the heat treatment of TiO_2 nanoparticles at 450 °C for 1 h results in slight sharpening of the anatase (101) reflection as a result of the growth of crystalline domains. However, TiO_2 particles in nanohybrid-I (Figure 2g) maintain their nanosized structure with an average diameter of 6.8 nm even after the heat treatment of 450 °C, suggesting that homogeneously distributed titanate nanosheets between TiO_2 nanoparticles inhibit a particle growth upon calcination (Table 1).

Table 1. Parameters Obtained from XRD Patterns and N_2 Adsorption−Desorption Measurements

sample	S_{BET}[a] ($m^2\ g^{-1}$)	V_t[b] (mL g^{-1})	V_{micro}[c] (mL g^{-1})	V_{meso} (mL g^{-1})	pore size[d] (nm)	particle size[e] (nm)
layered protonic titanate	13					
TiO_2 nanoparticle	100	0.097	0.035	0.062	1.8	9.1
microporous hybrid	250	0.171	0.153	0.018	1.0	
nanohybrid-I	190	0.367	0.060	0.307	6.3	6.8
nanohybrid-II	150	0.213	0.037	0.176	5.0	7.0

[a] BET specific surface area calculated from the linear part of teh BET plot. [b] V_t = total pore volume (taken from the volume of N_2 adsorbed at about $P/P_0 = 0.975$). [c] V_{micro} = micropore volume (estimated by the *t* plot). [d] The average pore diameter was estimated from the Barrett−Joyner−Halenda (BJH) formula, except for the microporous hybrid, in which the pore size is estimated from the micropore analysis method. [e] The average particle size of the heat-treated sample was evaluated by the Scherrer formula.

HRTEM Analysis. The nanohybrid samples embedded in epoxy resin were sliced by an ultramicrotome for the HRTEM observation. The as-synthesized nanohybrid-I (Figure 3a) exhibits two distinct images, lines and spherical shapes. The former are due to the exfoliated sheets of layered titanate whereas the latter are due to TiO_2 nanoparticles. Therefore, it becomes quite clear that loosely packed TiO_2 nanoparticles are hybridized with titanate nanosheets in such a way that the porous hybrid could be prepared. As seen in the TEM image of as-prepared nanohybrid-I, it is worth noting that the exfoliated titanate nanosheets are randomly hybridized with TiO_2 nanoparticles, which is in good agreement with the XRD results. The TEM image of nanohybrid-I calcined at 450 °C shows that this material is composed of spherically shaped crystallites with round edges (Figure 3b).

The samples exhibit lattice fringes corresponding to the (101) planes of the anatase phase as shown in magnified TEM images (Figure 3c,d). In case of as-prepared nanohybrid-I, an average particle size of anatase (6.1 ± 1.2 nm, 200 counts) is also in good agreement with that determined by XRD analysis using the Scherrer equation. The sample heated at 450 °C for 1 h shows the similar average particle size of 6.5 ± 1.4 nm (200 counts). It seems that randomly hybridized layered titanates inhibit particle growth upon calcination. Furthermore, as shown in Figure 3d, the exfo-

(18) Sasaki, T.; Watanabe, M. *J. Am. Chem. Soc.* **1998**, *120*, 4682.

(19) Cullity, B. D. *Elements of X-Ray Diffraction*, 2nd ed.; Addison-Wesley: Reading, MA, 1977.

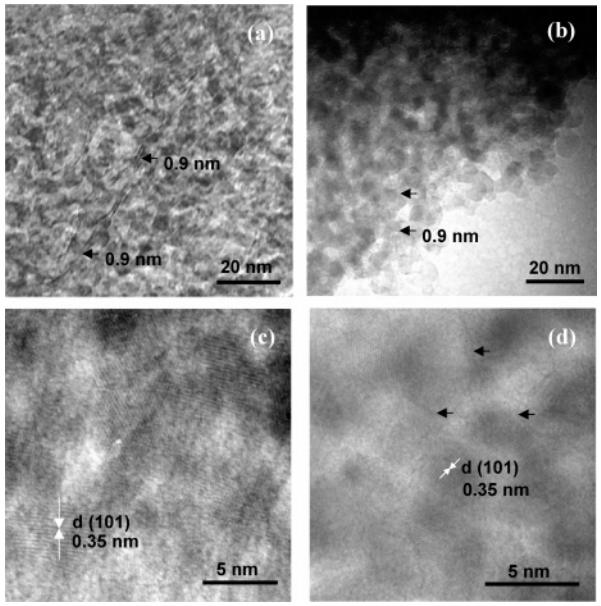

Figure 3. HRTEM images of (a) as-prepared nanohybrid-I, (b) calcined nanohybrid-I, (c) as-prepared nanohybrid-I (high magnification), and (d) calcined nanohybrid-I (high magnification). Black arrows denote the titanate nanosheets between TiO_2 nanoparticles.

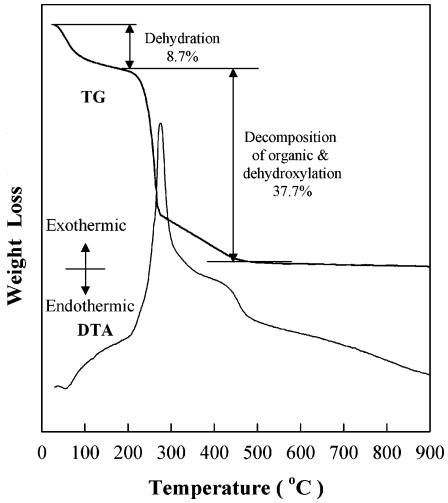

Figure 4. TG and DTA curves for nanohybrid-I.

liated nanosheets are still discernible partially between TiO_2 nanoparticles, and no reduction of interparticle distance could be seen even after calcinations, supporting that the nanohybrid sustains its porous structure. In the calcined sample, its crystallinity is slightly increased as a result of the surface curing during the heat treatment, which can be observed in the round shape of the particles.

Thermal Analysis. As shown in Figure 4, the TG-DTA curves for the nanohybrid-I can be divided into two temperature domains. The first weight loss below 150 °C is mostly attributed to the dehydration of water molecules,[20] and the second stronger weight loss with an exothermic peak between 150 and 450 °C is due to the decomposition of organic trace in the sample and the dehydroxylation. According to the thermal analysis, the thermal stability of mesoporous nanohybrid prepared in this way could be guaranteed at the temperature of 450 °C.

(20) Yin, S.; Uchida, S.; Fujishiro, Y.; Aki, M.; Sato, T. *J. Mater. Chem.* **1999**, *9*, 1191.

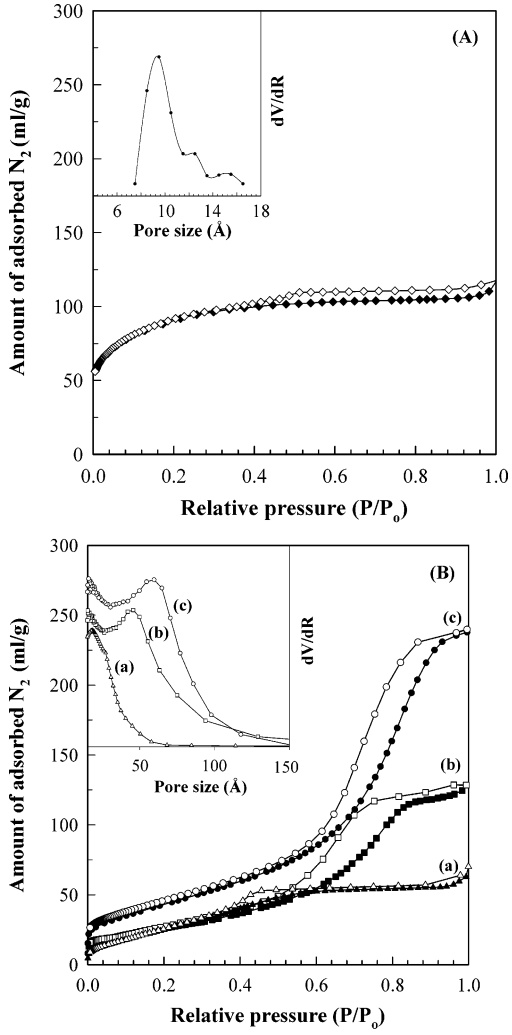

Figure 5. (A) Nitrogen adsorption−desorption isotherms for the microporous hybrid. (B) Nitrogen adsorption−desorption isotherms for (a) TiO_2 nanoparticles, (b) nanohybrid-II, and (c) nanohybrid-I. The inset indicates the pore size distribution curves, respectively.

Nitrogen Adsorption−Desorption Isotherms. As shown in the nitrogen adsorption−desorption isotherms (Figure 5), a drastic change in porosity can be seen by reassembling exfoliated titanate nanosheets with TiO_2 nanoparticles. According to the isotherm of TiO_2 nanoparticles, it can be classified into the type I based on the BDDT (Brunauer, Deming, Deming, and Teller) classification,[21,22] which is characteristic of microporous adsorbents. In addition, the adsorption−desorption isotherm for the microporous hybrid is type I and/or IV because of high microporosity. However, the nanohybrids show a fairly different type IV isotherm as a result of the mesoporosity. This result clearly reveals that the mesopores in the nanohybrids are developed by random hybridization of layered titanates with TiO_2 nanoparticles. The significant difference is also found in the hysteresis loop for the samples. The mesoporous nanohybrids show the type H3 hysteresis loop in the IUPAC classification,[21] suggesting that the slit-shaped pores are probably formed, whereas the nanoparticles and microporous hybrid show the type H4

(21) Allen, T. *Particle Size Measurement*, 5th ed.; Champman and Hall: London, 1997.
(22) Gregg, S. J.; Sing, K. S. W. *Adsorption, Surface Area, and Prorosity*, 2nd ed.; Academic: London, 1983.

indicative of typical microporous solids. As shown in Table 1, the BET specific surface area and porosities of nanohybrids increase drastically upon hybridization. The BET specific surface area is greatly enhanced from 13 m^2/g (layered protonic titanate) to 190 m^2/g (nanohybrid-I) upon hybridization. The total pore volume of nanohybrid-I (0.367 cm^3/g) is determined to be much larger than those of starting materials. It is worthwhile to note that the mesopore volume of nanohybrid-I is ~5 times higher than that of TiO_2 nanoparticles. In particular, the isotherms of mesoporous hybrid materials were fitted better by the BET equation than the Langmuir one as the relative pressure (P/P_0) is below 0.4, which means that the micropore does not significantly contribute to the total pore volume.

The pore size distribution curves of products calcined at 450 °C for 1 h is calculated by the BJH (Barrett, Joyner, and Halenda) method from the desorption branch (inset of Figure 5B).[20,21] For the comparison, the pore size distribution for the microporous hybrid is estimated by the micropore analysis method, which clearly shows that TiO_2-pillared titanate consists of micropores with an average size of 1.0 nm (inset of Figure 5A).[12,13] On the other hand, as shown in the pore size distribution curves, the pore size can be tailored within mesopore range by adjusting the ratio between titanate nanosheets and TiO_2 nanoparticles. The TiO_2 nanoparticle exhibits an average pore size of less than 2 nm resulted from a close packing of spherical nanoparticles. By increasing the content of layered titanate, mesopores with an average pore diameter of 6 nm were developed (nanohybrid-I), whereas the increase in the content of TiO_2 nanoparticles gave rise to the decrease in mesopores of 6 nm, with the simultaneous appearance of newly formed mesopores having the pore diameter of 5 nm due to the aggregation between TiO_2 nanoparticles (nanohybrid-II). Therefore, the optimal ratio to obtain the largest mesopore is found to be 1.5 in our system. The present mesopores of 5−6 nm can be clearly attributed to the spaces preserved by the TiO_2 nanoparticle (ca. 6 nm) existing between titanate nanosheets. As a consequence, the nanohybrids could allow organic molecules to easily access the entire surface of nanohybrids as a result of their mesoporosity developed by random hybridization, which results in the enhanced photocatalytic activity compared to the pristine materials such as TiO_2 nanoparticles or layered titanates. For that reason, the mesoporous nanohybrids, tailored by random hybridization, are expected to be much more efficient for photocatalysis of organic pollutants in comparison with the other materials such as microporous hybrid, layered titanate, and TiO_2 nanoparticle.

UV−Vis Diffuse Reflectance Spectra. Figure 6 shows the UV−vis diffuse reflectance spectra of nanohybrid-I in comparison with those of layered titanate derivatives and anatase TiO_2 nanoparticles. We investigated the origin of absorption variation by collecting the diffuse reflectance data and estimated band gap energies of the samples. The band gap energy (E_g) was calculated on the basis of a previously described method.[23] Briefly, an absorption coefficient (α) was calculated according to eq 1 (where R is the reflectance

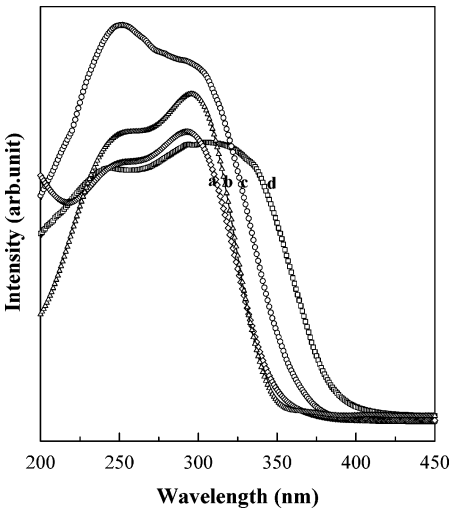

Figure 6. Diffuse UV−vis spectra for the layered protonic titanate (a, ◇), the layered cesium titanate (b, △), the nanohybrid-I (c, ○), and TiO_2 nanoparticle (d, □).

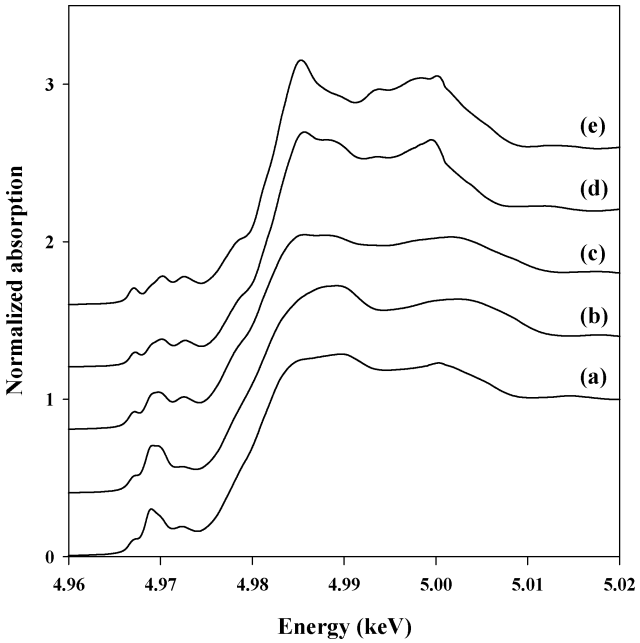

Figure 7. XANES spectra for (a) the layered protonic titanate, (b) the layered TBA-titanate, (c) as-prepared nanohybrid-I, (d) nanohybrid-I heat-treated at 450 °C for 1 h, and (e) crystalline bulk anatase TiO_2.

measured in UV−vis diffuse reflectance spectroscopy):

$$\alpha = -\ln(R) \tag{1}$$

Because the absorption coefficient is proportional to $F(R)$, the Kubelka−Munk function, a plot of $(F(R) \times h\nu)^{1/2}$ versus $h\nu$ (Supporting Information) gives a band gap energy for an indirect allowed transition.[24] The E_g for TiO_2 nanoparticles (~3.2 eV) agrees well with that of commercial bulk anatase TiO_2, suggesting that TiO_2 consists of agglomerated secondary particles after drying the colloidal TiO_2 nanosol. The layered cesium titanate and the layered protonic titanate exhibit a larger band gap of ~3.5 and ~ 3.4 eV, respectively, which is in good agreement with those of layered titanate

(23) Kavan, L.; Stoto, T.; Grätzel, M.; Fitzmaurice, D.; Shklover, V. *J. Phys. Chem.* **1993**, *97*, 9493.

(24) Salvador, P. *Sol. Energy Mater.* **1982**, *6*, 241.

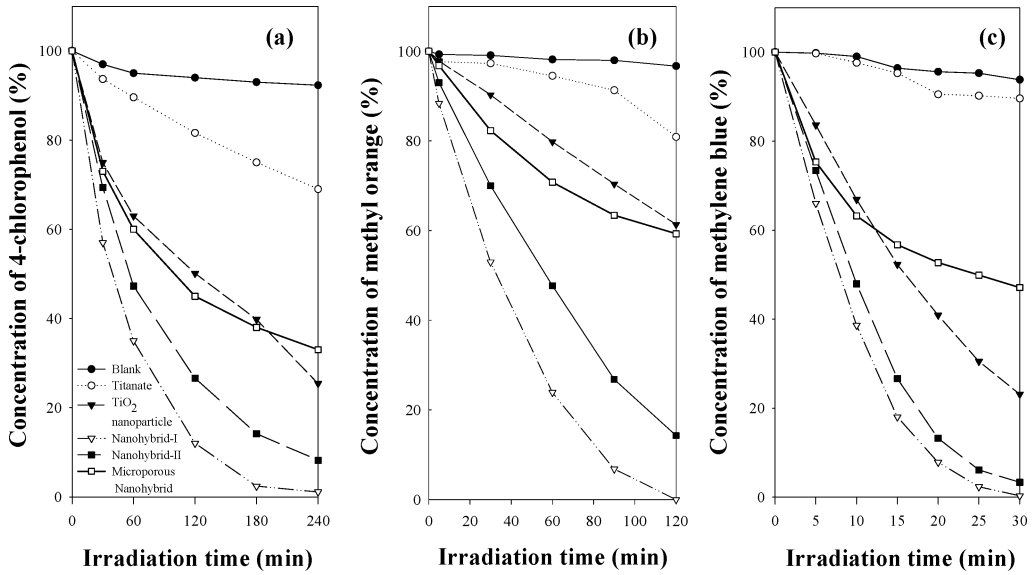

Figure 8. Catalytic performance of samples for photodegradation of (a) 4-CP, (b) MO, and (c) MB.

materials.[25] On the other hand, nanohybrid-I has a band gap energy of ~3.3 eV, which is rather blue-shifted compared to that of TiO_2 nanoparticles. As shown in the TEM image of nanohybrid-I, the titanate nanosheets exist between loosely packed TiO_2 nanoparticles. In such a porous structure, the titanate nanosheets seem to inhibit the agglomeration of TiO_2 particles. However, the E_g of the nanohybrid is red-shifted relative to that of the layered titanate, which might be attributed to the formation of bonds between the nanosheets and anatase TiO_2 nanoparticles upon hybridization.[13]

XANES. We also examined the XANES of the representative mesoporous nanohybrid-I along with the layered titanates and bulk anatase TiO_2, because the XANES analysis could provide useful information on the local structure around the titanium atom. The pre-edge region is strongly modulated by the surrounding atoms in an environment of short to medium range (<100 absorbing atoms) and, therefore, could provide structural and electronic information to understand the physicochemical properties of the present mesoporous nanohybrids. As shown in Figure 7, the XANES spectra of all the samples exhibit a pre-edge feature with three or four peaks followed by a white line one. These pre-edge peaks can be attributed to the forbidden transitions from the core 1s level to unoccupied 3d states of titanium atoms. The layered protonic titanate (Figure 7a) and the TBA-intercalated titanate (Figure 7b) show an intense peak around 4.969 keV in the pre-edge region, which is in good agreement with the previous literature value.[26,27] This is due to the severe distortion of TiO_6 octahedron in the layered titanate. However, after the hybridization between exfoliated nanosheets and TiO_2 nanoparticles, the central peak with high intensity at 4.968−4.969 keV is slightly suppressed in as-prepared nanohybrid-I (Figure 7c), and after heat-treatment at 450 °C for 1 h, the pre-edge peaks of nanohybrid-I (Figure 7d) are virtually similar to those of anatase TiO_2 (Figure 7e), suggesting that the severely distorted TiO_6 octahedra in the layered titanate might be homogeneously merged onto the surface of TiO_2 nanoparticles upon the heat treatment of 450 °C. Therefore, the local electronic structure for nanohybrid-I is analogous to that for the anatase TiO_2, which is quite desirable for efficient phocatalysis.

Photodegradation of Organic Pollutants. To explore photocatalytic properties of these mesoporous materials, we have investigated the photodegradation of 4-CP, MO, and MB over nanohybrid catalysts and host materials. Figure 8a shows the relative concentration of 4-CP as a function of time under UV irradiation. After 4 h of UV irradiation, 99% of 4-CP in an aqueous suspension was degraded over the nanohybrid-I catalyst. However, 75, 31, and 7% of 4-CP were degraded over catalysts such as TiO_2 nanoparticle, protonated layered titanate, and blank, respectively, at the same conditions. This result clearly shows that nanohybrid-I is a very effective catalyst for degradation of 4-CP. It is worthwhile to note here that only 67% of 4-CP was decomposed upon a microporous nanohybrid catalyst with a pore size of 1 nm.[13] In particular, the photocatalytic activity was affected not only from the surface area but also from the mesoporosity of titania because the reaction takes place not only on the external surface but also on the internal surface of titania catalyst.

Figure 8b illustrates the photocatalyzed disappearance of MO in the presence of various samples. From this study, it becomes more evident how important the mesoporosity of the catalyst would be in photocatalysis. After 2 h of irradiation, all the MO molecules were decomposed over the nanohybrid-I catalyst. On the other hand, the photodecomposition of MO on the microporous hybrid could be achieved only up to 40%. Such a difference in this study is not so surprising because the 4-CP molecules with a size of ~6.5 Å can be diffused into the pores of both the microporous hybrid and the mesoporous one. However, for the photodegradation of MO with such a larger molecular size (~15 Å), the mesoporous nanohybrid-I would be desirable as

(25) Kim, Y. I.; Atherton, S. J.; Brigham, E. S.; Mallouk, T. E. *J. Phys. Chem.* **1993**, *97*, 11802.
(26) Fukuda, K.; Nakai, I.; Oishi, C.; Nomura, M.; Harada, M.; Ebina, Y.; Sasaki, T. *J. Phys. Chem. B* **2004**, *108*, 13008.
(27) Fukuda, K.; Sasaki, T.; Watanabe, M.; Nakai, I.; Inaba, K.; Omote, K. *Cryst. Growth Des.* **2003**, *3*, 281.

confirmed by quite a high photocatalytic activity compared to the microporous hybrid with a restricted pore size. As shown in Figure 8c, we could observe the same photocatalytic decomposition behavior of MB. The mesopore size of 6 nm is large enough for the MB molecules to be accessed, because its molecular size is 15 Å, so that more effective reaction could occur in the mesopores of nanohybrids. It is, therefore, concluded that the pore size can be one of the most decisive factors in photocatalysis of organic molecules and that the present synthetic method is very efficient in fabricating the mesoporous catalysts by adjusting the ratio of nanoparticles to nanosheets, which can control the pore size. Furthermore, as confirmed by the XANES study, the local structure of the present mesoporous material, analogous to anatase TiO_2, is quite desirable for photocatalytic decomposition of organic pollutants.

Conclusion

This study clearly demonstrates that the hybridization of anatase nanoparticles with exfoliated titanate sheets could give rise to mesoporous nanohybrids and leads to an enhancement of photocatalytic activity. This new synthetic approach could be further expanded to the preparation of various semiconducting heterostructured materials with high surface area, controlled mesoporosity, and high thermal stability.

Acknowledgment. This work was supported by the Korean Research Foundation Grant (KRF-2004-041-C00187) and in part by the SRC program of the Korea Science and Engineering Foundation (KOSEF) through the Center for Intelligent Nano-Bio Materials at Ewha Womans University (Grant R11-2005-008-01001-0). The authors also thank the Ministry of Education for the Brain Korea 21 (BK21) fellowship. Dr. M. G. Kim is acknowledged for fruitful discussion of XANES results.

Note Added after ASAP Publication. There were errors in the anatase average particle sizes in the HRTEM analysis discussion in the version published ASAP February 3, 2006; the corrected version was published ASAP February 3, 2006.

Supporting Information Available: Details of the preparation method for the microporous hybrid, plots of $[F(R) \times h\nu]^{0.5}$ versus energy, and XRD analysis for microporous hybrid (PDF). This material is available free of charge via the Internet at http://pubs.acs.org.

CM052201D